# Millimeter-Wave Spatial Multiplexing in an Indoor Environment

Eric Torkildson, Colin Sheldon, Upamanyu Madhow, and Mark Rodwell
Department of Electrical and Computer Engineering
University of California, Santa Barbara
Santa Barbara, California 93106
Email: etorkild@ece.ucsb.edu

***Abstract*—A unique feature of communication at millimeter (mm) wave carrier frequencies is that spatial multiplexing is available for multiple-input multiple-output (MIMO) links with moderate antenna spacing even without a rich scattering environment. In this paper, we investigate the potential for exploiting this observation for increasing the spectral efficiency of indoor 60 GHz links. We begin by establishing limits on the spatial degrees of freedom available for linear antenna arrays of constrained length. A system architecture designed to exploit the available degrees of freedom, including beamforming as well as spatial multiplexing, is proposed. We evaluate the link capacity achievable by the proposed architecture when operating in a simple indoor environment. The results illustrate the relationship between between the channel quality and the relative positions of the transmit and receive nodes.**

## I. Introduction

Wireless transmission of high-definition (HD) multimedia signals is a topic of recent interest both in industry and the literature. The challenge in designing wireless links capable of this task stems from the high data rates that must be supported. In order to transmit an uncompressed 1080p HD video signal, for example, a wireless transmission scheme must support a data rate of at least 3.2 Gbps.

The mm-wave frequency bands present an attractive option for designing multigigabit wireless links because they offer an abundance of unlicensed or semi-unlicensed bandwidth. The unlicensed 60 GHz band, for example, offers 7 GHz of spectrum spanning 57 to 64 GHz in the United States. The opportunity for high data rate links at mm-wave frequencies is widely recognized: WirelessHD [1] and WiGig, for instance, represent industry-led efforts to define standard specifications for wireless interfaces capable of transmitting uncompressed HD multimedia signals at 60 GHz. Standardization efforts within the IEEE 802.15.3c and 802.11 task groups are provisioning for multimedia applications at 60 GHz as well. Meanwhile, the authors of [2] report a 6 Gbps link operating in the nearby 81-88 GHz band. Wired interfaces, however, continue to outpace their wireless counterparts. Version 1.3 of the wired High-Definition Multimedia Interface (HDMI) supports video resolutions as high as 1600p and data rates of up to 10.2 Gbps. For wireless links to close this gap, new wireless architectures are required.

With this motivation in mind, we investigate spatial multiplexing as a means to increase spectral efficiency at mm-wave frequencies. We first consider the spatial degrees of freedom that are available in a mm-wave LOS environment given linear arrays of constrained size. We find that the physical dimensions of common consumer electronic devices are sufficient to permit spatial multiplexing of several data streams at 60 GHz. We then describe a system architecture that exploits the available spatial degrees of freedom. The architecture, originally proposed in [3], employs a two-level hierarchical design that decouples the tasks of beamsteering and multiplexing at the transmitter. The performance of the proposed architecture, as measured by link capacity, is simulated assuming a simple indoor environment model. The results demonstrate that performance is dependent on the positioning of the transmit and receive nodes and existence of an unobstructed line-of-sight (LOS) path between them. We demonstrate that the impact of the node positions on performance can be reduced by increasing the number of antennas at the receive array.

This paper builds on an extensive body of MIMO literature that began with the work of Foschini [4] and Telatar [5]. The bulk of this literature has focused on spatial multiplexing at lower frequencies, for which a rich scattering environment is typically relied upon to produce a spatially uncorrelated wireless channel. At mm-wave frequencies, on the other hand, the LOS channel component usually dominates over multipath components due to relatively high reflection losses from many indoor building materials [6]. As a result, antenna array geometry and positioning, which determine the LOS channel component, become critical factors in determining the suitability of a mm-wave channel for spatial multiplexing. The LOS channel is modeled here using a simple ray-tracing approach, although numerous other viable channel models exist. An overview of common indoor channel models is provided in [7].

The capacity of an indoor 60 GHz MIMO link was previously studied in [8]. The authors considered relatively small inter-antenna spacings ($2\lambda$, where $\lambda$ is the carrier wavelength) whereas in this work, we leverage prior results showing that a

This research was supported in part by the National Science Foundation under grants ECS-0636621, CCF-0729222, CNS-0520335, and CNS-0832154.

larger antenna separation (i.e. on the order of $\sqrt{R\lambda}$, where $R$ is link distance) is optimal for achieving spatial multiplexing gains over a LOS channel [9]. Additionally, greater emphasis is placed on illustrating link performance as a function of node position within the environment.

The paper is organized as follows. In Section II, we describe a simple indoor environment and channel model. We proceed to estimate the potential of a LOS MIMO link to achieve spatial multiplexing gains given array length constraints. In Section II-B, we describe a simple architecture that realizes this potential under optimal conditions (i.e. perfect array alignment and optimal distance between nodes). The performance of this architecture in the previously described indoor environment is assessed in Section IV. It is demonstrated that the positioning of the nodes and the existence of a LOS path between the nodes are critical factors determining channel quality. Concluding remarks and future work are included in Section V.

## II. Spatial Degrees of Freedom Under a Linear Array Length Constraint

We begin this section by describing the physical indoor wireless environment and corresponding channel model that will be used throughout this paper. We then demonstrate that, given array length constraints appropriate to indoor applications, there is significant potential for spatial multiplexing gains at mm-wave frequencies.

### A. Channel Model

We consider a two-node mm-wave link operating in a simple indoor environment. The transmit node represents a signal source (e.g. cable box, laptop, etc.) and has a length of $L_1 = \frac{1}{3}$ m (we disregard its height, as we consider only two dimensions herein). It is equipped with an $N_T$ element linear array of length $L_T \leq L_1$. The receive node (e.g. HD display) has a length of $L_2 = 1$ m. It possesses a linear array of $N_R$ elements and length $L_R \leq L_2$. The two nodes are placed in room of dimensions $w \times 8$ m and are aligned parallel with the front and back walls as illustrated in Figure 1. The receive node is centered at the fixed coordinates $(\frac{w}{2}, 0)$, while the coordinates of the transmit node are variable and given by $(x, y)$ with $0 < x < w$ and $0 < y < 8$.

The $N_R \times 1$ received vector $\mathbf{y}$ is given by

$$\mathbf{y} = \mathbf{H}\mathbf{x} + \mathbf{w} \qquad (1)$$

where $\mathbf{H}$ represents the $N_R \times N_T$ channel matrix, $\mathbf{x}$ is the $N_T \times 1$ transmitted signal vector, $\mathbf{w}$ is an $N_R \times 1$ additive white complex Gaussian noise vector with covariance $\mathbf{C_w} = N_0 \mathbf{I}_{N_R}$, and $\mathbf{I}_{N_R}$ is the $N_R \times N_R$ identity matrix.

The channel matrix $\mathbf{H}$ is modeled using a ray-tracing approach that includes LOS paths and rays reflected once of either side wall. Higher order reflections are disregarded in this simulation due to the additional path loss and reflection loss they incur, as well as the directionality of the antennas to be considered. While we focus on 60 GHz links throughout this paper, the results can be extended to other frequencies (e.g. 70-80-90 GHz bands) as long as the LOS channel components dominate over multipath. Restricting attention to narrowband signals, we model the channel as

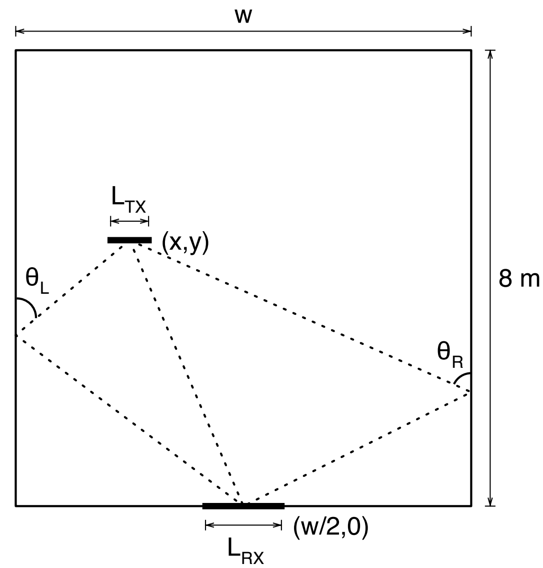


Fig. 1. Top-down view of indoor environment illustrating LOS and single reflection paths.

$$\mathbf{H} = \mathbf{H}_{LOS} + \mathbf{H}_R + \mathbf{H}_L \qquad (2)$$

where $\mathbf{H}_{LOS}$, $\mathbf{H}_R$, and $\mathbf{H}_L$ are the contributions of the LOS path, right wall reflected path, and left wall reflected path, respectively. The $(m, n)$th entry of $\mathbf{H}_{LOS}$, representing the complex gain from the $n$th transmit antenna to the $m$th receive antenna, is given by

$$\begin{aligned} h_{LOS}(m,n) &= \frac{p_{LOS}(1,1)}{p_{LOS}(m,n)} e^{\left(-i\frac{2\pi}{\lambda} p_{LOS}(m,n)\right)} && (3) \\ &\approx e^{\left(-i\frac{2\pi}{\lambda} p_{LOS}(m,n)\right)} && (4) \end{aligned}$$

where $\lambda$ is the wavelength of the carrier wave and $p_{LOS}(m, n)$ is the LOS path length between the $n$th transmit antenna and $m$th receive antenna. Note that the transmit power has been normalized by a factor of $p_{LOS}(1, 1)$ so that the LOS contribution to the channel gain maintains approximately unity power irrespective of the position of the transmit node. The $(m, n)$th entries of $\mathbf{H}_R$ and $\mathbf{H}_L$ are given by

$$h_R(m,n) = \Gamma(\theta_R) \frac{p_{LOS}(1,1)}{p_R(m,n)} e^{\left(-i\frac{2\pi}{\lambda} p_R(m,n)\right)} \qquad (5)$$

and

$$h_L(m,n) = \Gamma(\theta_L) \frac{p_{LOS}(1,1)}{p_L(m,n)} e^{\left(-i\frac{2\pi}{\lambda} p_L(m,n)\right)} \qquad (6)$$

respectively, where $p_R(m, n)$ $(p_L(m, n))$ is the length of the path from the $n$th transmit antenna to the point of reflection on the right (left) wall and then to the $m$th receive antenna. The angles of incidence off the right and left walls are given by $\theta_R$ and $\theta_L$ respectively. An expression for $\Gamma(\theta)$, the perpendicular Fresnel reflection coefficient, can be found in [6].

### B. Size-Based Limit on Spatial Multiplexing

A MIMO channel offers a degree-of-freedom gain when the spatial dimension is exploited. This is achieved through spatial multiplexing, which permits simultaneous transmission of multiple data streams. Using the singular value decomposition of the channel matrix $\mathbf{H}$, Telatar demonstrated that the MIMO channel can be decomposed into parallel, non-interfering single-input, single-output (SISO) channels [5]. The channel gains are specified by the singular values of $\mathbf{H}$, denoted by $\sigma_i$ with $i = 1, \ldots, \min(N_T, N_R)$. The distribution of the singular values and the method of transmit power allocation determine how many of the available spatial channels provide adequate gain to support data streams.

It is known that the antenna array geometry, the number of antennas, and the scattering environment are limiting factors to number of spatial degrees of freedom [10]. At lower frequencies, a rich scattering environment is critical to producing a spatially uncorrelated channel conducive to multiplexing. At 60 GHz and above, however, multipath is attenuated by high reflection loss and cannot be relied upon to provide an uncorrelated channel. Fortunately, the carrier wavelength at these frequencies is small enough that moderate separation between antenna elements is sufficient to allow multiplexing, even in purely LOS environments [3] [9].

To characterize the multiplexing capability of the indoor link, we seek the maximum number of spatial channels that can be achieved given a constrained array size. We assume that a linear array of half-wavelength spaced antenna elements extends across the entire length of each node. We consider a carrier frequency of 60 GHz with a wavelength of $\lambda = 5$ mm. There are then $N_T = \lfloor \frac{2L_T}{\lambda} \rfloor = 134$ elements in the transmit array and $N_R = \lfloor \frac{2L_R}{\lambda} \rfloor = 403$ elements in the receive array, where $\lfloor x \rfloor$ is the largest integer less than or equal to $x$. To derive a result independent of a specific physical environment, we consider only the LOS component $\mathbf{H}_{LOS}$ of the channel response. We observe that some singular values of $\mathbf{H}_{LOS}$ are orders of magnitude larger than the rest. These represent the spatial channels over which data can be transmitted reliably. We define a singular value as dominant if $\sigma_i^2 > N_R$. Figure 2 plots the number of dominant singular values as a function of link range, assuming the two arrays are aligned to the broadside of one another. We observe at least ten dominant singular values over the range of interest.

This result is consistent with the wavevector-aperture product, a measure of degrees of freedom of a MIMO link proposed by Poon *et al.* [10]. The wavevector-aperture product is $\min(|\mathcal{A}_T||\Omega_T|, |\mathcal{A}_R||\Omega_R|)$, where $\mathcal{A}_T$ ($\mathcal{A}_R$) is the effective aperture of the transmit (receive) antenna array scaled by wavelength, and $|\Omega_T|$ ($|\Omega_R|$) is the angular spread of the physical environment in solid angle as seen by the transmitter (receiver). Specializing to the given scenario, we have $|\mathcal{A}_T| = L_T/\lambda$, $|\mathcal{A}_R| = L_R/\lambda$, $|\Omega_T| = 2\tan^{-1}\left(\frac{L_R}{2R}\right)$, and $|\Omega_R| = 2\tan^{-1}\left(\frac{L_T}{2R}\right)$, where $R$ is the link range. The degrees of freedom as given by the wavevector-aperture product are plotted in Fig. 2.

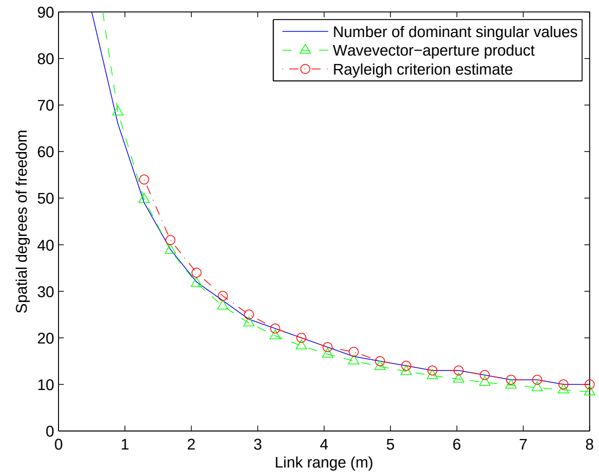


Fig. 2. Spatial degrees of freedom in a LOS environment given linear arrays of lengths $L_T = 1/3$ m and $L_R = 1$ m. and a carrier frequency of 60 GHz

## III. Example mm-Wave MIMO System

In the previous section, we demonstrated that numerous spatial degrees of freedom are attainable in a LOS environment using linear antenna arrays constrained in length to the physical dimensions of typical consumer electronics. However, the arrays under consideration consisted of an impractically large number of antenna elements. In this section, we demonstrate that the number of antenna elements can be reduced significantly while preserving all available degrees of freedom by using optimal antenna spacing. We then consider an example mm-wave MIMO architecture that applies this result.

### A. Optimal Array Configurations

When $N$ and $R$ are known, the inter-antenna spacing of a uniform linear array (ULA) can be chosen such that the columns of $\mathbf{H}_{LOS}$ (the receive array responses to various transmit elements) are orthogonal. This array configuration maximizes the LOS channel capacity. The minimum spacing that achieves this condition is given by the Rayleigh spacing criterion:

$$d_T d_R = \frac{R\lambda}{N} \tag{7}$$

where $d_T$ is the distance between adjacent transmit array elements and $d_R$ is the distance between adjacent receive array elements [9] [3].

Array lengths are given by $L_T = d_T(N-1)$ and $L_R = d_R(N-1)$. By substituting these values into (7) and solving for $N$, we produce an alternate estimate of the maximum number of degrees of freedom available over a LOS channel given an array length constraint. This yields

$$\begin{aligned} N &= \frac{1}{2}\lfloor 2 + \frac{L_T L_R}{R\lambda} + \sqrt{\left(2 + \frac{L_T L_R}{R\lambda}\right)^2 - 2^2} \rfloor & (8) \\ &\approx \lfloor \frac{L_T L_R}{R\lambda} + 2 \rfloor & (9) \end{aligned}$$

TABLE I
LENGTHS OF RAYLEIGH-SPACED ULAS OPTIMIZED FOR A 60 GHZ CARRIER AND $R = 5$ M

| $N$ | 2 | 3 | 4 | 5 | 6 |
|---|---|---|---|---|---|
| $d$ (cm) | 11.1 | 9.1 | 7.9 | 7.0 | 6.4 |
| $L$ (cm) | 11.1 | 18.2 | 23.7 | 28.0 | 32.0 |

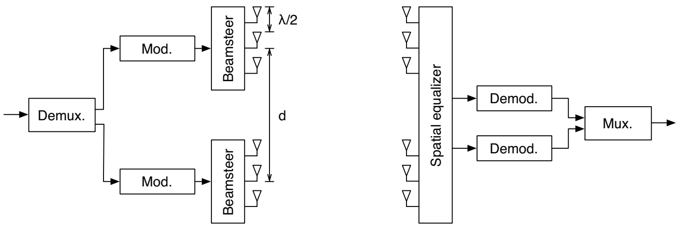


Fig. 3. Example mm-wave MIMO architecture. $M$-element subarrays provide directivity, while the array of subarrays provides spatial multiplexing gains.

Due to approximations used in deriving the Rayleigh spacing criterion, this estimate holds only when $R > \max(L_T, L_R)$. $N$ is plotted for $L_T = 1/3$ m, $L_R = 1$ m, and 1.3 m $\leq R \leq 8$ m in Fig. 2, where it is referred to as the Rayleigh criterion estimate. We observe that a Rayleigh-spaced array offers $N$ degrees of freedom using $N$ antennas per array.

Fig. 2 indicates that ten or more spatial eigenmodes are available to our example 60 GHz link. In practice, however, cost and complexity considerations, rather than array size, may be the limiting factors determining a link's multiplexing capability. Assuming $d_T = d_R = d$, Table I lists the optimal inter-element spacing $d$ and overall array length $L$ for arrays of two to six elements. The arrays have been optimized for a link range of 5 m and a carrier frequency of 60 GHz according to (7).

The optimal antenna spacing assumes the link range $R$ is known and fixed. In practice, however, the link should operate reliably throughout the indoor environment. The performance of the link over a variable link range is considered in Section IV.

### B. Example System Architecture

We now describe a mm-wave architecture that performs beamsteering and spatial multiplexing in a two-level hierarchical fashion. Each array has $N$ elements separated by distance $d$ chosen according to (7). Each element is actually a half-wavelength spaced $M$-antenna subarray, which can be implemented as a monolithic microwave integrated circuit (MMIC). This array-of-subarrays approach provides the necessary directivity to attenuate unwanted reflections from grating lobes when the LOS path is present. On the other hand, if the LOS path is blocked, the subarrays can be used to beamsteer the signal along reflected paths. Figure 3 depicts a $2 \times 2$ link with $M = 3$.

The transmitter, which has limited knowledge of the channel, sends a single data stream from each subarray. The transmitter subarrays obey a linear phase profile and are thus limited to beamsteering in a given direction. At the receiver, full channel state information is assumed. The receiver recovers a noisy estimate of the two transmitted signals using spatial equalization, i.e. a zero-forcing (ZF) or minimum mean-squared error (MMSE) filter, BLAST, etc. Although modern receivers often perform channel estimation and equalization in the digital domain, such an approach here would require $NM$ high-speed, high-precision analog-to-digital converters. If a linear spatial equalizer (i.e. ZF or MMSE) is used, however, spatial equalization can be performed using analog hardware prior to digitization. This approach, which lowers the number of high-speed ADCs and relaxes their performance requirements, has been demonstrated using a four-channel hardware prototype in [11].

The input to the spatial equalizer is given by

$$\mathbf{y} = \mathbf{HAs} + \mathbf{w} = \hat{\mathbf{H}}\mathbf{s} + \mathbf{w} \tag{10}$$

where $\mathbf{s}$ is an $N \times 1$ data vector, $\mathbf{A}$ is an $NM \times N$ steering matrix, and $\hat{\mathbf{H}} = \mathbf{HA}$ is an $NM \times N$ equivalent channel matrix combining the propagation environment and the steering matrix. $\mathbf{A}$ is given by

$$\mathbf{A} = \begin{bmatrix} e^{-i\pi\cos(\theta_1)} & 0 \\ \vdots & \vdots \\ e^{-i\pi M\cos(\theta_1)} & 0 \\ 0 & e^{-i\pi\cos(\theta_2)} \\ \vdots & \vdots \\ 0 & e^{-i\pi M\cos(\theta_2)} \end{bmatrix} \tag{11}$$

where $\theta_i$ is the direction in which the $i$th subarray is steering. Given a linear spatial equalizer, the equalizer output is

$$\mathbf{r} = \mathbf{C}^H\mathbf{y} = \mathbf{C}^H\left(\hat{\mathbf{H}}\mathbf{s} + \mathbf{w}\right) \tag{12}$$

where equalizer coefficients are given by $\mathbf{C}$. We will assume herein a linear MMSE equalizer with coefficients given by

$$\mathbf{C}_{\text{MMSE}} = \left(\sigma_b^2\hat{\mathbf{H}}\hat{\mathbf{H}}^H + N_0\mathbf{I}_{NM}\right)^{-1}\sigma_b^2\hat{\mathbf{H}} \tag{13}$$

where $\sigma_b^2 = \frac{P}{NM}$ is the per-antenna transmit power assuming equal power allocation and $P$ is a total power constraint. The signal to interference and noise ratio (SINR) at the $k$th output of the equalizer is given by

$$\gamma_k = \frac{\sigma_b^2|\mathbf{c}_k^H\hat{\mathbf{H}}_k|^2}{\sigma_b^2\sum_{j\neq k}|\mathbf{c}_j^H\hat{\mathbf{H}}_k|^2 + N_0\mathbf{c}_k^H\mathbf{c}_k} \tag{14}$$

where $\mathbf{c}_k$ is the $k$th column of $\mathbf{C}_{\text{MMSE}}$.

The capacity of this system, given the constraints of equal transmit power and linear MMSE spatial equalization, is given by

$$\mathcal{C} = \sum_{k=1}^{N}\log_2\left(1 + \gamma_k\right) \tag{15}$$

The capacity is the maximum rate of communication per unit bandwidth for which the error probability can be made arbitrarily small. In the following section, we will compute the capacity when this architecture is paired with the indoor environment model of Section II-A.

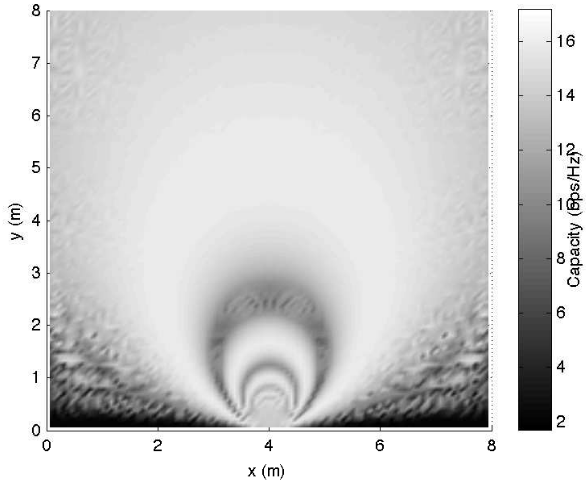


Fig. 4. Capacity as a function of transmitter position for the $2 \times 2$ system.

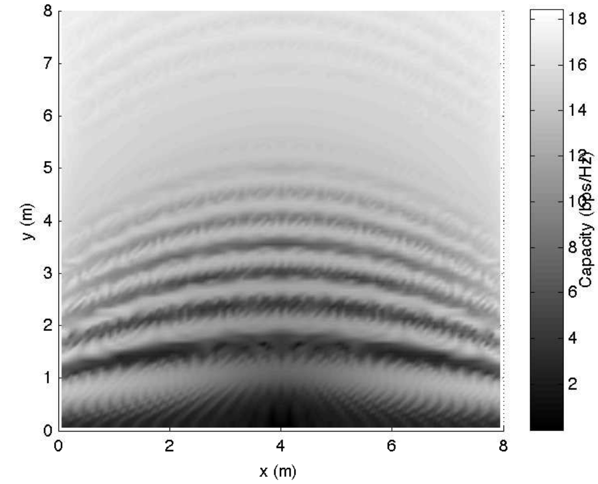


Fig. 5. Capacity as a function of transmitter position when the LOS path is blocked for the $2 \times 2$ link. To compensate for reflection loss, transmit power has been increased by 10 dB.

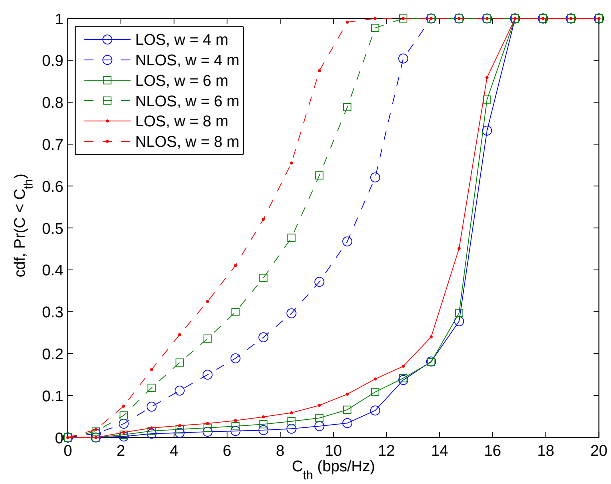


Fig. 6. CDF of the link capacity assuming uniform random placement of the transmit node. The distance separating the front and back walls is 8 m, while the distance separating the side walls is given by $w$. LOS indicates that the line-of-sight path is available and NLOS indicates that it is not. Transmit power is increased by 10 dB in the NLOS cases.

## IV. Numerical Results

In this section, we compute the channel capacity given by (15) assuming the proposed architecture operates in the environment described in Section II-A. We assume $N = 2$ subarrays per node separated by $d = 0.11$ m, which is optimal at link range $R = 5$ m according to (7). We assume each subarray consists of $M = 5$ half-wavelength spaced antenna elements. $P/N_0$ is 10 dB. The reflection coefficient is computed using a complex dielectric constant of $\epsilon = \epsilon_r - j\sigma\lambda$, where $\epsilon = 4.44$ and $\sigma = 0.001$ are chosen as suitable parameters to model plasterboard walls [8]. The dimensions of the room are 8 m by 8 m. The receiver is centered at coordinates (4, 0) m and the capacity is calculated when the transmitter is centered at coordinates $(x, y)$ with 0 m $< x, y < 8$ m.

Fig. 4 plots the channel capacity as a function of the transmit array coordinates. The transmitter beamsteers each signal in the direction that maximizes capacity. This generally results in steering both signals along the LOS path to the receiver. However, the LOS component of the channel matrix becomes ill-conditioned at certain positions (e.g., positions indicated by dark rings), leading to a drop in capacity. At some of these positions, steering one or both beams in the direction of reflected paths increases capacity.

If the LOS path between the transmitter and receiver is blocked, the channel quality may be degraded significantly. We model this scenario by removing the LOS component from the channel matrix, resulting in $\mathbf{H} = \mathbf{H}_L + \mathbf{H}_R$. Fig. 5 plots the capacity assuming a non line-of-sight (NLOS) channel. The transmit power has been increased by 10 dB to offset reflection losses. The channel quality is highly dependent on the transmitter position when the LOS path is blocked.

Fig. 6 plots the cumulative distribution function (CDF) of the capacity assuming the transmitter coordinates $(x, y)$ are chosen at random. Results are also provided when $w$, the distance separating the side walls, is reduced to 4 m and 6 m. We observe that when the LOS path is unobstructed, the capacity is largely independent of $w$ due to the dominance of the LOS component in the channel model. When the LOS path is blocked, however, the capacity is inversely proportional to $w$. This is due to an increased average path length and angle of incidence when the distance between the side walls is increased.

We further observe from Fig. 6 that there is a positive probability that the capacity will go nearly to zero when the LOS path is blocked. This occurs when the transmitter attempts to multiplex $N$ signals over a channel with fewer than $N$ non-zero eigenvalues. In this case, it would be preferable to transmit a single data stream from each set of highly-correlated

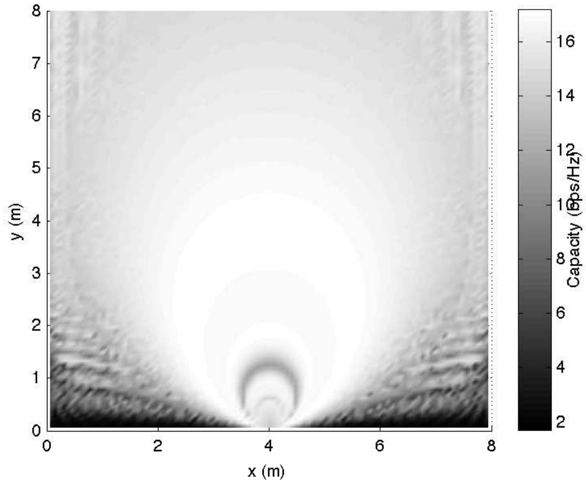


Fig. 7. Capacity as a function of transmitter position for the $2 \times 3$ system.

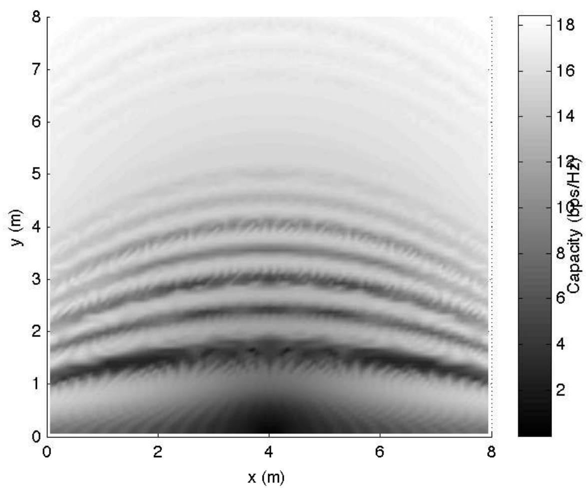


Fig. 8. Channel capacity as a function of transmitter position when the LOS path is blocked for the $2 \times 3$ link. To compensate for reflection loss, transmit power has been increased by 10 dB.

subarrays.

In order to improve the robustness of the link, the receiver may be equipped with additional antennas/subarrays. This will decrease the probability of the LOS component of the channel response from becoming ill-conditioned. To illustrate, we modify the receiver by placing a third subarray between the original two subarrays. The channel capacity of this $2 \times 3$ link is plotted as a function of transmitter position in Fig. 7. Spatial correlation is reduced in the LOS component of the modified channel matrix. As a result, link performance is less dependent on the positioning of the transmit and receive nodes when the LOS path is available. In the NLOS scenario, plotted in Fig. 8, the effect of the additional receive subarray is less pronounced.

## V. Conclusion

Our simulation results indicate that spatial multiplexing at 60 GHz is feasible in an indoor MIMO environment. Although the channel capacity is sensitive to the relative positions of the nodes, we have demonstrated that this sensitivity can be reduced by increasing the number of antennas at the receiver. The proposed system architecture, which relies on limited channel knowledge at the transmitter (i.e. knowledge of the directions of the LOS and reflected paths), can successfully multiplex data streams across the spatial dimension in the environment considered here.

In this work, we restricted attention to a narrowband channel. However, the 60 GHz band is characterized by its abundant bandwidth. Assuming multigigabit signaling over a large bandwidth, the delay spread due to the multipath components can grow to 10s of symbols in length. Wideband system design and performance calculations are topics for future work.

It was shown that the channel degradation can be significant when the LOS path is blocked due to an obstruction. In future work, more accurate and elaborate channel models and simulated environments can be used to better assess link performance in the absence of a LOS path. Further, various array geometry effects, including co-polarization patterns, phase patterns, and non-isotropic gain, can be considered.

## References

[1] J. Gilbert, C. Doan, S. Emami, and C. B. Shung, "A 4-Gbps uncompressed wireless HD A/V transceiver chipset," *IEEE Micro*, vol. 28, no. 2, pp. 56–64, March 2008.

[2] V. Dyadyuk, J. Bunton, J. Pathikulangara, R. Kendall, O. Sevimli, L. Stokes, and D. Abbott, "A multigigabit millimeter-wave communication system with improved spectral efficiency," *Microwave Theory and Techniques, IEEE Transactions on*, vol. 55, no. 12, pp. 2813–2821, Dec. 2007.

[3] E. Torkildson, B. Ananthasubramaniam, U. Madhow, and M. Rodwell, "Millimeter-wave MIMO: Wireless links at optical speeds," in *Proc. of 44th Allerton Conference on Communication, Control and Computing*, September 2006.

[4] G. J. Foschini and M. Gans, "On the limits of wireless communications in a fading environment when using multiple antennas," *Wireless Personal Communications*, vol. 6, no. 3, p. 311, Mar. 1998.

[5] I. E. Telatar, "Capacity of multi-antenna Gaussian channels," AT&T Bell Lab Internal Tech. Memo., Oct. 1995.

[6] P. F. M. Smulders, "Deterministic modelling of indoor radio propagation at 40-60 Ghz," *Wireless Personal Communications*, vol. 4, no. 2, pp. 127–135, June 1994.

[7] C. Hofmann, A. Knopp, D. Ogermann, R. Schwarz, and B. Lankl, "Deficiencies of common mimo channel models with regard to indoor line-of-sight channels," in *Personal, Indoor and Mobile Radio Communications, 2008. PIMRC 2008. IEEE 19th International Symposium on*, Sept. 2008, pp. 1–6.

[8] A. Arvanitis, G. Anagnostou, N. Moraitis, and P. Constantinou, "Capacity study of a multiple element antenna configuration in an indoor wireless channel at 60 ghz," in *Vehicular Technology Conference, 2007. VTC2007-Spring. IEEE 65th*, April 2007, pp. 609–613.

[9] F. Bohagen, P. Orten, and G. Oien, "Design of optimal high-rank line-of-sight MIMO channels," *Wireless Communications, IEEE Transactions on*, vol. 6, no. 4, pp. 1420–1425, April 2007.

[10] A. Poon, R. Brodersen, and D. Tse, "Degrees of freedom in multiple-antenna channels: a signal space approach," *Information Theory, IEEE Transactions on*, vol. 51, no. 2, pp. 523–536, Feb. 2005.

[11] C. Sheldon, M. Seo, E. Torkildson, M. Rodwell, and U. Madhow, "Four-channel spatial multiplexing over a millimeter-wave line-of-sight link," *IEEE - MTTS International Microwave Symposium*, June 2009.